

# A Solution-Processable Polymer Photocatalyst for Hydrogen Evolution from Water

Duncan J. Woods, Reiner Sebastian Sprick, Charlotte L. Smith, Alexander J. Cowan, and Andrew I. Cooper\*

Direct photocatalytic water splitting is an attractive strategy for clean energy production, but multicomponent nanostructured systems that mimic natural photosynthesis can be difficult to fabricate because of the insolubility of most photocatalysts. Here, a solution-processable organic polymer is reported that is a good photocatalyst for hydrogen evolution from water, either as a powder or as a thin film, suggesting future applications for soluble conjugated organic polymers in multicomponent photocatalysts for overall water splitting.

The direct production of hydrogen from water using solar energy could be an important technology to meet future energy demands. Sunlight is an abundant energy source that can be stored in dihydrogen molecules, which have a high gravimetric energy density. Semiconductors with an appropriate bandgap are required to harvest solar energy, and to facilitate hydrogen evolution from water. Such materials can either be used as part of photoelectrochemical (PEC) cells<sup>[1–3]</sup> or as direct photocatalysts in aqueous suspensions.<sup>[4]</sup> Direct photocatalysis has the advantage of being technologically simple and having a lower projected cost.<sup>[5]</sup>

A large number of inorganic photocatalysts have been studied for hydrogen evolution.<sup>[6–9]</sup> By contrast, organic photocatalysts are much less explored, despite possible advantages such as tunable bandgaps, synthetic control over structure, good processability, and preparation from earth-abundant materials.<sup>[10,11]</sup> The most widely studied organic-derived photocatalysts for hydrogen evolution are the family of materials known as “graphitic carbon nitrides” (g-C<sub>3</sub>N<sub>4</sub>). Graphitic carbon nitrides were shown to

exhibit photocatalytic hydrogen evolution in 2009,<sup>[12]</sup> and many advances have been made since then.<sup>[13,14]</sup> After the potential of g-C<sub>3</sub>N<sub>4</sub> was first observed, while focusing on the hydrogen evolution half-reaction, interest has begun to shift to achieving overall water splitting using these materials.<sup>[15,16]</sup> However, the exact structure of most g-C<sub>3</sub>N<sub>4</sub> materials is unknown and the synthesis usually involves high temperature processing, which offers limited scope for fine-tuning structure and properties.

Also, while g-C<sub>3</sub>N<sub>4</sub> can be produced from inexpensive starting materials, the synthetic yield of the material is typically low.<sup>[15,17]</sup> Of special relevance here, graphitic carbon nitrides are insoluble solids: as for many inorganic catalysts, this can present challenges in terms of processing.

Rather few organic photocatalysts have been studied for hydrogen evolution other than g-C<sub>3</sub>N<sub>4</sub>. Recently, nitrogen-containing poly(azomethine) networks and covalent triazine-based frameworks (CTFs) were shown to have photocatalytic activity with the addition of platinum cocatalysts.<sup>[18,19]</sup> We have shown that a series of conjugated microporous polymers (CMPs) could facilitate hydrogen evolution from water in the presence of a sacrificial electron donor, without any additional heavy metal cocatalyst.<sup>[20,21]</sup> Other CMPs have since been studied for photocatalysis<sup>[22,23]</sup> and recent studies have demonstrated that linear conjugated polymers can have high photocatalytic activities.<sup>[24,25]</sup> However, as with g-C<sub>3</sub>N<sub>4</sub>, none of these organic materials are soluble in common organic solvents. This insolubility makes it more challenging to process these materials into functional composites. Moreover, photocatalysts are typically kept in suspension by stirring to prevent sedimentation, which results in loss of photocatalytic activity.<sup>[26]</sup> The loss of activity of insoluble catalysts can be prevented with the use of support substrates,<sup>[27]</sup> however, using solution processability allows the use of simpler supports and easier development of photoelectrodes.

Soluble oligo(phenylene)s have been previously reported as photocatalysts, however, they displayed low activity, were only active under UV light, required a Ru cocatalyst and were only poorly soluble in organic solvents limiting processability.<sup>[28]</sup> More recently soluble metal-chelating polymers have been prepared although the photocatalytic activity of these polymers also appear to be very low with apparent quantum yields (AQY) below  $3 \times 10^{-4}\%$ .<sup>[29]</sup> The solubility of some alkylated conjugated polymers has also facilitated the preparation of polymer nanoparticles (PDots).<sup>[30,31]</sup> The preparation of these PDots enabled significant enhancements in rate over the pristine polymer although scalability and long-term stability of this approach has yet to be shown.

D. J. Woods, Dr. R. S. Sprick, C. L. Smith,  
Dr. A. J. Cowan, Prof. A. I. Cooper  
Department of Chemistry  
University of Liverpool  
Crown Street, Liverpool L69 7ZD, UK  
E-mail: aicooper@liverpool.ac.uk

D. J. Woods, Dr. R. S. Sprick, Prof. A. I. Cooper  
Materials Innovation Factory  
51 Oxford Street, Liverpool L7 3NY, UK

C. L. Smith, Dr. A. J. Cowan  
Stephenson Institute for Renewable Energy  
University of Liverpool  
Chadwick Building, Peach Street, Liverpool L69 7ZF, UK

© 2017 The Authors. Published by WILEY-VCH Verlag GmbH & Co. KGaA, Weinheim. This is an open access article under the terms of the Creative Commons Attribution License, which permits use, distribution and reproduction in any medium, provided the original work is properly cited.

The copyright line for this article was changed on 7 Nov 2017 after original online publication.

DOI: 10.1002/aenm.201700479

We report here a well-defined soluble organic polymer that photocatalyzes the evolution of hydrogen from water in the presence of a sacrificial electron donor with no added metal cocatalyst. We demonstrate that despite the low molecular weight of the soluble fraction of the polymer, high rates of hydrogen evolution are maintained relative to the higher molecular weight insoluble fraction. We hypothesize that this solubility could open up a range of opportunities that are not available with insoluble photocatalyst materials, such as the use of solution processing for the scalable preparation of nanocomposites (e.g., an organic hydrogen-evolving polymer film with an embedded inorganic oxygen-evolving catalyst). Also, soluble polymers might be cast as films and used as part of a PEC cell or in an “artificial leaf” architecture.<sup>[32]</sup>

Alkyl side chains are commonly used to make solution-processable conjugated polymers for organic photovoltaic devices.<sup>[33]</sup> We selected the insoluble polymer (poly[(9*H*-carbazole-2,7-diyl)-1,4-phenylene]) (**P4**) as a starting point because we showed previously that **P4** has good photocatalytic activity.<sup>[24]</sup> Also, the carbazole nitrogen in **P4** offers scope for alkylation to produce soluble analogs. Addition of the 2-ethylhexyl side chain yielded the polymer **P8** (Figure 1a). We used this side chain because branched alkyl chains give rise to greater solubility enhancements compared to equivalent linear chains.<sup>[33]</sup>

Polymer **P8** was synthesized via Suzuki–Miyaura polycondensation of 1,4-benzenediboronic acid bis(pinacol) ester and 2,7-dibromo-9-(2-ethylhexyl)-9*H*-carbazole in toluene with Na<sub>2</sub>CO<sub>3</sub> (0.2 M), Aliquat 336, and [Pd(PPh<sub>3</sub>)<sub>4</sub>] in toluene at

80 °C.<sup>[34]</sup> After 48 h, the reaction mixture was extracted with toluene and the organic products were further purified using Soxhlet extraction in methanol, acetone, and ethyl acetate. The chloroform-soluble fraction of the 2-ethylhexyl-substituted polymer, **P8-s**, was recovered and reprecipitated into methanol. A higher molecular weight chloroform-insoluble fraction of the polymer, **P8-i**, was also obtained.<sup>[35]</sup> All other fractions contained only trace amounts of product and were therefore discarded.

Fourier-transform infrared spectroscopy (FT-IR) demonstrated the presence of the expected alkyl C–H functionalities (2800–3000 cm<sup>-1</sup>) and absence of any unsubstituted carbazole N–H (3400–3500 cm<sup>-1</sup>) for both **P8-i** and **P8-s** (Figure S2, Supporting Information). In fact, the FT-IR spectra of **P8-i** and **P8-s** appear to be essentially identical, suggesting that they have analogous structures and differ only in terms of molecular weight. The solubility of **P8-s** allowed us to characterize it by <sup>1</sup>H NMR spectroscopy (Figure S4, Supporting Information). This spectrum shows the aliphatic protons of the 2-ethylhexyl side chain (1.4–1.7 ppm) as well as the aromatic signals (7.7–8.1 ppm) in the expected ratio. The molecular weight of **P8-s** was determined to be *M*<sub>w</sub> = 2100 g mol<sup>-1</sup> (*M*<sub>n</sub> = 1500 g mol<sup>-1</sup>; Đ = 1.4) by gel permeation chromatography analysis calibrated against polystyrene standards.

UV–Visible and photoluminescence (PL) spectroscopy were used to probe the optoelectronic properties of these materials. Figure 1c,d shows the UV–vis and PL spectra of **P8-s** as a powder, as a chloroform solution, and as a cast film. The absorption spectra of the **P8-s** film and powder are similar,

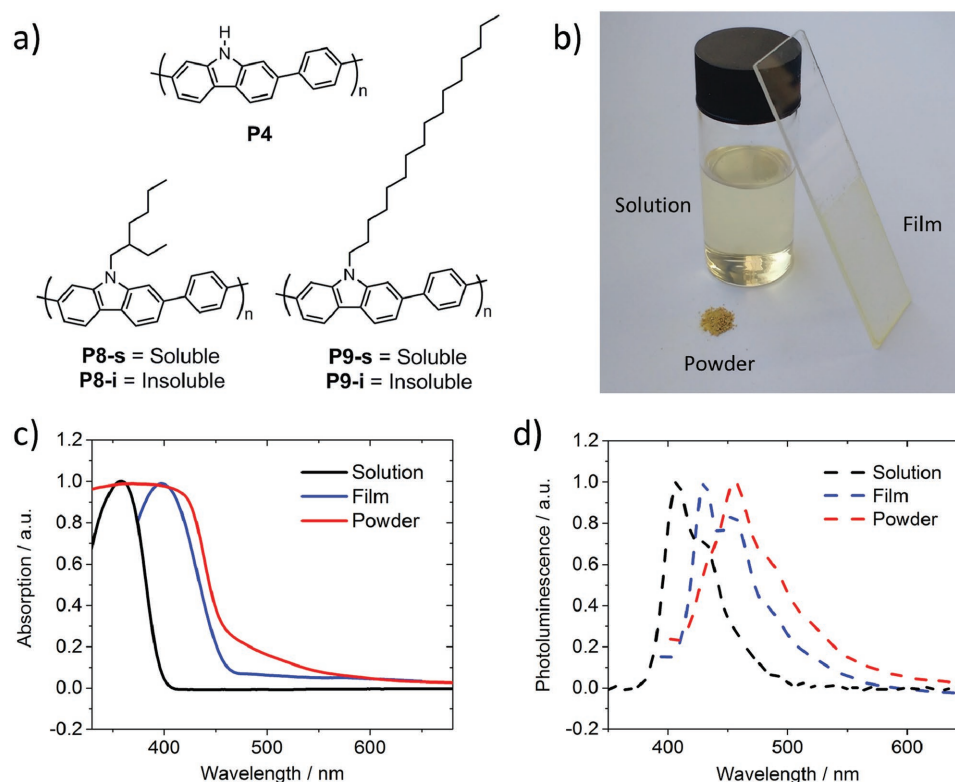


**Figure 1.** a) Structures of **P4**, **P8**, and **P9** (solubility here refers to solubility in chloroform). b) Photograph of **P8-s** as a powder, in chloroform solution, and as a drop cast film. c) UV–vis absorption and d) photoluminescence ( $\lambda_{\text{exc}} = 360$  nm) spectra of **P8-s** as a powder, cast as a film, and dissolved in chloroform.

as expected, with optical gaps of 2.79 eV for the film and 2.71 eV for the powder. However, a significant blue shift is observed for the polymer in solution, probably due to the loss of  $\pi$ - $\pi$  stacking between chains.<sup>[36]</sup> The PL spectra for the film (430 nm) and powder (455 nm) are red shifted compared to the solution maximum (407 nm). Powder samples of the insoluble **P8-i** fraction displayed similar absorption and emission profiles to powdered **P8-s** (Figures S6 and S7, Supporting Information). Powder X-ray diffraction (PXRD) patterns of **P8-s** and **P8-i** both show limited degrees of crystallinity (Figure S16, Supporting Information). Thermogravimetric analysis shows that both **P8-s** and **P8-i** were stable up to temperatures of around 300 °C in air (Figure S18, Supporting Information).

The photocatalytic activity of the materials for hydrogen evolution from water in the presence of triethylamine (TEA) as a sacrificial electron donor was studied. In addition, methanol was used in the aqueous mixture to enhance miscibility of TEA with water, and to improve wettability of the hydrophobic polymer.<sup>[24]</sup> When acetonitrile was used instead of methanol as a cosolvent in the TEA/water mixture, a comparable hydrogen evolution rate was observed (**P8-i**, Figure S22, Supporting Information). Negligible hydrogen evolution was observed when methanol alone was used as a sacrificial electron donor, and no hydrogen evolution was observed for pure water (**P8-i**, Figure S23, Supporting Information). **P8-i** powder evolves hydrogen from the water/methanol/TEA mixture with a rate of 21.5  $\mu\text{mol h}^{-1}$  (860  $\mu\text{mol g}^{-1} \text{h}^{-1}$ ) under  $\lambda > 295$  nm irradiation, while powdered **P8-s** produced 13.6  $\mu\text{mol h}^{-1}$  (544  $\mu\text{mol g}^{-1} \text{h}^{-1}$ ) under the same conditions in suspension (see Table 1).

It appears that the introduction of the 2-ethylhexyl side chain in **P8-i** and **P8-s** does not affect the hydrogen evolution rate greatly with respect to our previous insoluble polymer,<sup>[24]</sup> **P4** – indeed, the catalytic activity for **P8-i** is somewhat higher than for **P4** under  $\lambda > 295$  nm irradiation. An analogous polymer, **P9**, with the longer, unbranched hexadecyl side chain was found to be significantly lower than that of **P8** for both soluble and insoluble fractions (Figures S24 and S25, Supporting

Information). Contact angle measurements showed **P9-s** to be more hydrophobic than **P8-s** (Table S4, Supporting Information) and it follows that the longer, more hydrophobic alkyl side chains seem to decrease the wettability and dispersity of **P9** in the water/methanol/TEA mixture used for hydrogen evolution. PXRD patterns also showed **P9-s** and **P9-i** to be less crystalline than **P8-s** and **P8-i** (Figures S16 and S17, Supporting Information) which may also account for their reduced hydrogen evolution activities.

A strong dependency on the illumination wavelength was found for hydrogen evolution experiments of **P8-s** and the AQY was estimated for **P8-s** to be 0.56% at  $\lambda = 420$  nm (Figure S37, Supporting Information). Analysis of palladium content by inductively coupled plasma optical emission spectrometry shows the palladium content of **P8-s** to be 0.02% compared to 0.50% for **P8-i**. Residual palladium has been suggested to act as cocatalysts in photocatalytic hydrogen evolution in covalent triazine-based frameworks,<sup>[37]</sup> and in conjunction with  $\text{g-C}_3\text{N}_4$ .<sup>[38]</sup> Low thresholds for the effect of residual palladium on the photocatalytic performance has been reported in conjugated microporous polymers,<sup>[22]</sup> and for Au loaded onto La-doped  $\text{NaTaO}_3$ .<sup>[39]</sup> It is unclear whether the amount of residual palladium, difference in molecular weight, crystallinity, hydrophobicity or a combination of all of these factors affect the photocatalytic performance in comparison to **P8-i**.

Extended hydrogen evolution runs were performed for **P8-s** under  $\lambda > 420$  and 295 nm irradiation and using a solar simulator (Figures S27–S29, Supporting Information). After 92.5 h under  $\lambda > 295$  nm irradiation and with intermittent degassing, **P8-s** evolved 328  $\mu\text{mol}$  of  $\text{H}_2$ . The polymer showed good stability according to FT-IR,  $^1\text{H}$  NMR, UV–vis, and PL spectroscopy (Figures S31–S33, Supporting Information).

The soluble and insoluble fractions of **P8**, **P8-s**, and **P8-i**, have slightly different photocatalytic performances. **P8-i** showed superior performance under irradiation at both  $\lambda > 295$  nm and  $\lambda > 420$  nm, possibly because of its higher molecular weight. This is interesting in the context of other recent findings: for example, branched phenyl triazine oligomers were shown to have higher photocatalytic activities than the equivalent extended covalent triazine-based framework (CTF-1).<sup>[40]</sup> By contrast, increased molecular weights in linear semiconducting polymers have been shown to give higher charge carrier mobilities.<sup>[41]</sup> The relationship between the degree of polymerization and photocatalytic performance appears, therefore, to be system-dependent. However, the fact that **P8-s** still evolves hydrogen at a comparable rate to **P8-i** with such a low molecular weight suggests that only limited effective conjugation lengths are required for photocatalysis.

An advantage of soluble, linear polymers over branched phenyl-triazine oligomers<sup>[40]</sup> or oligo(phenylene)s<sup>[42]</sup> is that they can form coherent films with reasonable mechanical strength. Initially, we prepared a film of **P8-s** by drop casting from chloroform solution onto a glass slide. However, when this slide was immersed in the water/methanol/TEA mixture, partial delamination of the film occurred.

This problem was circumvented when **P8-s** (0.34 mg) was drop cast from chloroform onto mesoporous  $\text{SnO}_2$ . This gave a more stable film with better adherence to the slide. Irradiation of the film immersed in the water-splitting medium ( $\lambda > 295$  nm

**Table 1.** Summary of solubility in chloroform, hydrogen evolution rates, and optical gap of **P8-s** and **P8-i** in comparison to **P4** and commercially available  $\text{g-C}_3\text{N}_4$ <sup>[24]</sup> and  $\text{TiO}_2$ .

Photocatalyst	Solubility in $\text{CHCl}_3$	$\text{HER}^{\text{a}}$ > 420 nm [ $\mu\text{mol h}^{-1}$ ]	$\text{HER}^{\text{a}}$ > 295 nm [ $\mu\text{mol h}^{-1}$ ]	Optical gap <sup>b</sup> ) [eV]
<b>P4</b>	Insoluble	5.6 ( $\pm 0.2$ )	13.8 ( $\pm 0.2$ )	2.72
<b>P8-s</b>	Soluble	1.8 ( $\pm 0.03$ )	13.6 ( $\pm 0.2$ )	2.71
<b>P8-i</b>	Insoluble	3.1 ( $\pm 0.02$ )	21.5 ( $\pm 0.1$ )	2.77
<b>P9-s</b>	Soluble	0.5 ( $\pm 0.01$ )	2.0 ( $\pm 0.05$ )	2.49
<b>P9-i</b>	Insoluble	0.9 ( $\pm 0.04$ )	3.2 ( $\pm 0.04$ )	2.94
$\text{g-C}_3\text{N}_4$	Insoluble	2.7 ( $\pm 0.1$ )	11.2 ( $\pm 0.6$ )	2.70
$\text{TiO}_2$	Insoluble	0.1 ( $\pm 0.003$ )	37.3 ( $\pm 1.3$ )	3.13

<sup>a</sup>) Reaction conditions (i) Polymers: 25 mg of photocatalyst (**P8-s**, **P8-i** or **P4**) suspended in water/methanol/TEA solution, irradiated using 300 W Xe lamp for 5 h using the stated band pass filter (no additional Pt added). (ii)  $\text{g-C}_3\text{N}_4$  (commercial grade): 25 mg photocatalyst suspended in 10 vol% triethanolamine in water loaded with 3 wt% Pt. (iii)  $\text{TiO}_2$ : 25 mg photocatalyst suspended in water/methanol/TEA solution with photodeposition of 1 wt% Pt; <sup>b</sup>) Calculated from the onset of the absorption spectrum, see the Supporting Information.

filter) resulted in the evolution of 0.66  $\mu\text{mol}$  of hydrogen after 5 h (hydrogen evolution rate of 450  $\mu\text{mol g}^{-1} \text{h}^{-1}$ , Figure S30, Supporting Information). The slide was removed and the degassed solution was irradiated once more ( $\lambda > 295 \text{ nm}$  filter) to determine if any delamination of the polymer had taken place during the irradiation. The rate of hydrogen evolution was reduced by almost a factor of ten, confirming that the polymer film on the slide was chiefly responsible for hydrogen evolution and only a small amount of delamination had occurred. No hydrogen evolution was observed from the uncoated  $\text{SnO}_2$  slide under the same irradiation conditions. Clearly, further work is needed to optimize the film preparation and to prepare a completely stable film. Nevertheless, this is the first example, to the best of our knowledge, of direct photocatalytic hydrogen evolution from water using a solution-processed organic polymer film.

Transient absorption (TA) spectroscopic measurements could also be performed on films of **P8-s** as a result of their minimal scattering. TA spectroscopy can provide useful insight into lifetimes of excited states, quenching, and the role of solvents in the reaction mixture. **Figure 2** shows TA spectra of **P8-s** films on glass following 365 nm excitation. In water, photoinduced absorptions (PIAs) are observed immediately after excitation at 524, 564, 648 nm, with a broad feature at 740 nm also being present on the approximate timescale of the instrument response ( $\approx 0.6 \text{ ps}$ , Figure 2a). The TA spectral features initially decay rapidly with  $t_{50\%}$  (the time for 50% of the PIA at  $\approx 1 \text{ ps}$  to decay by 50%) being  $\approx 2 \text{ ps}$ , leaving a small

( $\approx 10\%$  of the original) PIA that persists beyond the maximum timescale observable (3.1 ns) in this experiment (Figure 2a,c). Experiments in water and methanol (1:1) (Figure S38, Supporting Information) show similar behavior, with only a slight increase in excited state lifetime ( $t_{50\%} \approx 4 \text{ ps}$ ), confirming that the primary role of the methanol is not as sacrificial electron donor. This is in line with the hydrogen evolution experiments, which required TEA to yield significant levels of  $\text{H}_2$  (vide supra). In contrast, in the presence of both methanol and TEA (Figure 2b), a more pronounced rapid decay of the initially formed PIAs at 524, 564, and 648 nm occurs. Simultaneously, a long-lived, very broad absorption ( $t_{50\%} \approx 50 \text{ ps}$ , Figure 2c) grows in with a maximum at  $\approx 700 \text{ nm}$  with a shoulder at 570 nm (Figure S39, Supporting Information), which persists beyond 3.1 ns (Figure S40, Supporting Information). The long lifetime of this spectral feature in the presence of the sacrificial electron donor, coupled to its dissimilarity to previously reported spectra of positive polarons of related poly(carbazole)s<sup>[43]</sup> leads us to tentatively assign it to an electron polaron state, formed by the rapid ( $< 2 \text{ ps}$ ) quenching of the excitonic state in the presence of the sacrificial electron donor, TEA (Figure 2d).

In summary, we have prepared a polymeric conjugated photocatalyst that can be processed in solution to form photocatalytically active thin films. This material also demonstrates good photocatalytic performance and photostability in suspension. TA spectroscopy studies give insights into excited state dynamics and their timescales, allowing for understanding of

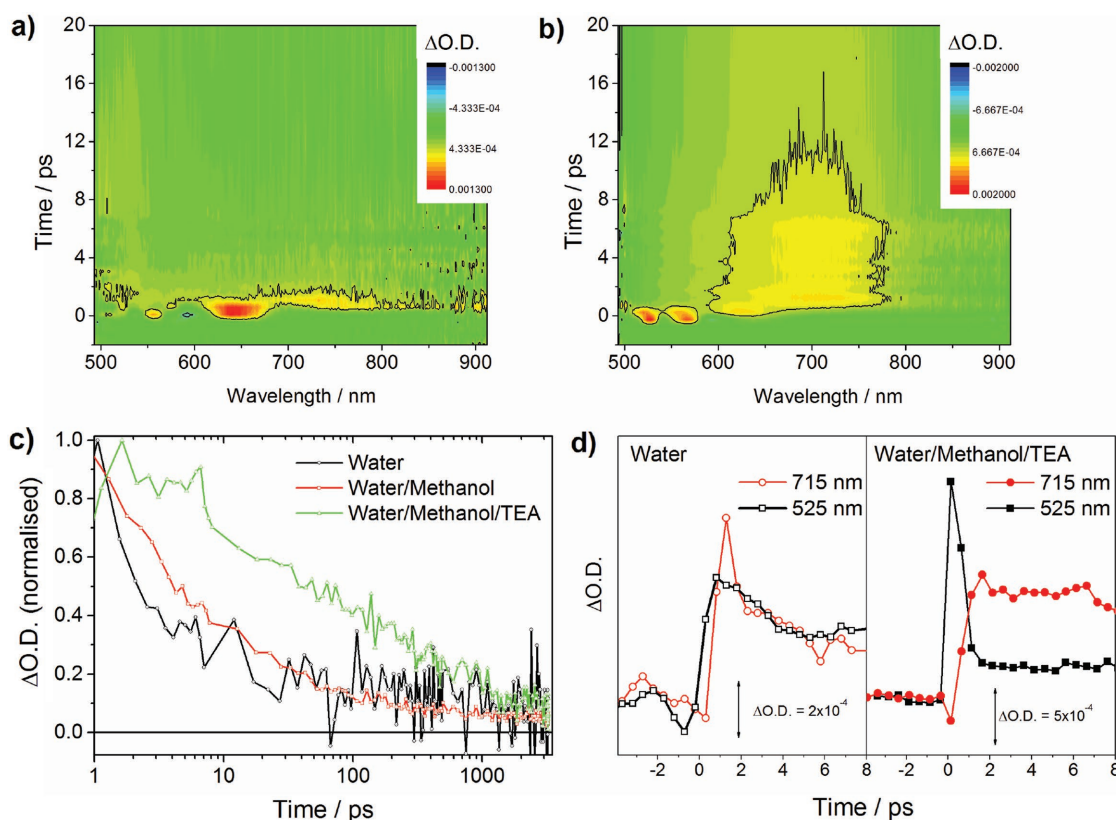


**Figure 2.** a) TA spectra of **P8-s** following 365 nm excitation in water and b) water/methanol/TEA (1:1:1). c) Kinetic traces recorded at 715 nm in the solvent indicated showing an increase in transient lifetime following the addition of the primary hole scavenger (TEA). d) Kinetics recorded at 715 and 525 nm showing the rapid quenching of the 525 nm feature in the presence of TEA to give rise to a long-lived photoinduced absorption.

the roles played by each component of the system. Furthermore, we have evidence for electron transfer from the amine scavenger onto the photolytically formed exciton state forming an electron polaron state.

Solution processing opens several directions that are more challenging with insoluble catalysts. For example, fabrication of large-scale photocatalytic devices on flexible supports by established printing techniques, e.g., inkjet or roll-to-roll printing.<sup>[44]</sup> Moreover, the solubility of **P8-s** should also enable the facile preparation of nanoparticles. Nanoparticles of  $\pi$ -conjugated polymers have generated a great deal of interest in recent years as a result of their excellent fluorescent properties.<sup>[45,46]</sup> By greatly decreasing the particle size of these soluble materials, we might be able to achieve better optical penetration of light (i.e., reduced scattering) and enhanced hydrogen evolution rates, as has recently been achieved with other soluble polymer photocatalysts.<sup>[30]</sup> More generally, overall water splitting without any sacrificial hole or electron scavengers may require more than one photocatalyst, and we anticipate that solution processability might open up routes to new composite photocatalysts in the future.

## Supporting Information

Supporting Information is available from the Wiley Online Library or from the author.

## Acknowledgements

The authors thank the Engineering and Physical Sciences Research Council (EPSRC) for financial support under Grants EP/N004884/1 and EP/K006851/1. The Laser Loan Pool of the Central Laser Facility (CLF), part of the UK Science and Technology Facilities Council (STFC), is thanked for the loan of equipment through EP/G03088X/1. The authors also thank J. Lee and F. Jäckel for assistance with TA experiments, R. Clowes for performing SEM, Prof. K. Durose for access to the profilometer, and Dr. K. Doherty for performing contact angle measurements.

## Conflict of Interest

The authors declare no conflict of interest.

## Keywords

conjugated polymers, organic, photocatalysis, soluble, solution processable

Received: February 22, 2017

Revised: June 30, 2017

Published online: September 1, 2017

- [1] E. Lanzarini, M. R. Antognazza, M. Biso, A. Ansaldo, L. Laudato, P. Bruno, P. Metrangolo, G. Resnati, D. Ricci, G. Lanzani, *J. Phys. Chem. C* **2012**, *116*, 10944.
- [2] F. Fumagalli, S. Bellani, M. Schreier, S. Leonardi, H. Comas-Rojas, A. Ghadirzadeh, G. Tullii, A. Savoini, G. Marra, L. Meda, M. Grätzel, G. Lanzani, M. T. Mayer, M. R. Antognazza and F. Di Fonzo, *J. Mater. Chem. A* **2015**, *4*, 2178.

- [3] K. Sivula, R. van de Krol, *Nat. Rev. Mater.* **2016**, *1*, 15010.
- [4] C.-H. Liao, C.-W. Huang, J. C. S. Wu, *Catalysts* **2012**, *2*, 490.
- [5] D. M. Fabian, S. Hu, N. Singh, F. A. Houle, T. Hisatomi, K. Domen, F. E. Osterloh, S. Ardo, *Energy Environ. Sci.* **2015**, *8*, 2825.
- [6] X. Chen, S. Shen, L. Guo, S. S. Mao, *Chem. Rev.* **2010**, *110*, 6503.
- [7] Y. Li, G. Chen, Q. Wang, X. Wang, A. Zhou, Z. Shen, *Adv. Funct. Mater.* **2010**, *20*, 3390.
- [8] D. Praveen Kumar, M. V. Shankar, M. M. Kumari, G. Sadanandam, B. Srinivas, V. Durgakumari, *Chem. Commun.* **2013**, *49*, 9443.
- [9] O. Rosseler, M. V. Shankar, M. K. Le Du, L. Schmidlin, N. Keller, V. Keller, *J. Catal.* **2010**, *269*, 179.
- [10] C. J. Brabec, *Sol. Energy Mater. Sol. Cells* **2004**, *83*, 273.
- [11] G. Zhang, Z.-A. Lan, X. Wang, *Angew. Chem.* **2016**, *128*, 15940; *Angew. Chem. Int. Ed.* **2016**, *55*, 15712.
- [12] X. Wang, K. Maeda, A. Thomas, K. Takanabe, G. Xin, J. M. Carlsson, K. Domen, M. Antonietti, *Nat. Mater.* **2009**, *8*, 76.
- [13] X. Fan, L. Zhang, R. Cheng, M. Wang, M. Li, Y. Zhou, J. Shi, *ACS Catal.* **2015**, *5*, 5008.
- [14] K. Schwinghammer, M. B. Mesch, V. Duppel, C. Ziegler, J. Senker, B. V. Lotsch, *J. Am. Chem. Soc.* **2014**, *136*, 1730.
- [15] J. Liu, Y. Liu, N. Liu, Y. Han, X. Zhang, H. Huang, Y. Lifshitz, S.-T. Lee, J. Zhong, Z. Kang, *Science* **2015**, *347*, 970.
- [16] Y. Zhang, E. Zhao, H. Deng, J. W. Y. Lam, B. Z. Tang, *Polym. Chem.* **2016**, *7*, 2492.
- [17] D. J. Martin, P. J. T. Reardon, S. J. A. Moniz, J. Tang, *J. Am. Chem. Soc.* **2014**, *136*, 12568.
- [18] M. G. Schwab, M. Hamburger, X. Feng, J. Shu, H. W. Spiess, X. Wang, M. Antonietti, K. Müllen, *Chem. Commun.* **2010**, *46*, 8932.
- [19] J. Bi, W. Fang, L. Li, J. Wang, S. Liang, Y. He, M. Liu, L. Wu, *Macromol. Rapid Commun.* **2015**, *36*, 1799.
- [20] R. S. Sprick, J.-X. Jiang, B. Bonillo, S. Ren, T. Ratvijitvech, P. Guigliion, M. A. Zwiijnenburg, D. J. Adams, A. I. Cooper, *J. Am. Chem. Soc.* **2015**, *137*, 3265.
- [21] V. S. Vyas, B. V. Lotsch, *Nature* **2015**, *521*, 41.
- [22] L. Li, Z. Cai, Q. Wu, W. Y. Lo, N. Zhang, L. X. Chen, L. Yu, *J. Am. Chem. Soc.* **2016**, *138*, 7681.
- [23] R. S. Sprick, B. Bonillo, M. Sachs, R. Clowes, J. R. Durrant, D. J. Adams, A. I. Cooper, *Chem. Commun.* **2016**, *52*, 10008.
- [24] R. S. Sprick, B. Bonillo, R. Clowes, P. Guigliion, N. J. Brownbill, B. J. Slater, F. Blanc, M. A. Zwiijnenburg, D. J. Adams, A. I. Cooper, *Angew. Chem.* **2016**, *128*, 1824; *Angew. Chem. Int. Ed.* **2016**, *55*, 1792.
- [25] C. Yang, B. C. Ma, L. Zhang, S. Lin, S. Ghasimi, K. Landfester, K. A. I. Zhang, X. Wang, *Angew. Chem.* **2016**, *128*, 9348; *Angew. Chem. Int. Ed.* **2016**, *55*, 9202.
- [26] M. Schwarze, D. Stellmach, M. Schröder, K. Kailasam, R. Reske, A. Thomas, R. Schomäcker, *Phys. Chem. Chem. Phys.* **2013**, *15*, 3466.
- [27] M. Schröder, K. Kailasam, J. Borgmeyer, M. Neumann, A. Thomas, R. Schomäcker, M. Schwarze, *Energy Technol.* **2015**, *3*, 1014.
- [28] S. Yanagida, T. Ogata, Y. Kuwana, Y. Wada, K. Murakoshi, A. Ishida, S. Takamuku, M. Kusaba, N. Nakashima, *J. Chem. Soc., Perkin Trans. 2* **1996**, *0*, 1963.
- [29] L. Li, R. G. Hadt, S. Yao, W. Y. Lo, Z. Cai, Q. Wu, B. Pandit, L. X. Chen, L. Yu, *Chem. Mater.* **2016**, *28*, 5394.
- [30] L. Wang, R. Fernández-Terán, D. L. A. Fernandes, L. Tian, H. Chen, H. Tian, *Angew. Chem.* **2016**, *128*, 12494; *Angew. Chem. Int. Ed.* **2016**, *55*, 1.
- [31] P. B. Pati, G. Damas, L. Tian, D. Fernandes, L. Zhang, I. B. Pehlivan, T. Edvinsson, C. M. Araujo, H. Tian, *Energy Environ. Sci.* **2017**, *10*, 1372.
- [32] D. G. Nocera, *Acc. Chem. Res.* **2012**, *45*, 767.

- [33] J. Mei, Z. Bao, *Chem. Mater.* **2014**, *26*, 604.
- [34] F. Dierschke, A. C. Grimsdale, K. Müllen, *Synthesis* **2003**, *16*, 2470.
- [35] B. A. Miller-Chou, J. L. Koenig, *Prog. Polym. Sci.* **2003**, *28*, 1223.
- [36] A. B. Koren, M. D. Curtis, A. H. Francis, J. W. Kampf, *J. Am. Chem. Soc.* **2003**, *125*, 5040.
- [37] C. B. Meier, R. S. Sprick, A. Monti, P. Guiglion, J.-S. M. Lee, M. A. Zwijnenburg, A. I. Cooper, *Polymer* **2017**; <https://doi.org/10.1016/j.polymer.2017.04.017>.
- [38] K. Maeda, K. Domen, *J. Phys. Chem. Lett.* **2010**, *1*, 2655.
- [39] A. Iwase, H. Kato, A. Kudo, *Appl. Catal., B* **2013**, *136–137*, 89.
- [40] K. Schwinghammer, S. Hug, M. B. Mesch, J. Senker, B. V. Lotsch, *Energy Environ. Sci.* **2015**, *8*, 3345.
- [41] M. Tong, S. Cho, J. T. Rogers, K. Schmidt, B. B. Y. Hsu, D. Moses, R. C. Coffin, E. J. Kramer, G. C. Bazan, A. J. Heeger, *Adv. Funct. Mater.* **2010**, *20*, 3959.
- [42] S. Matsuoka, H. Fujii, T. Yamada, C. Pac, A. Ishida, S. Takamuku, M. Kusaba, N. Nakashima, S. Yanagida, *J. Phys. Chem.* **1991**, *95*, 5802.
- [43] C. Huang, M. M. Sartin, M. Cozzuol, N. Siegel, S. Barlow, J. W. Perry, S. R. Marder, *J. Phys. Chem. A* **2012**, *116*, 4305.
- [44] R. Søndergaard, M. Hösel, D. Angmo, T. T. Larsen-Olsen, F. C. Krebs, *Mater. Today* **2012**, *15*, 36.
- [45] C. Wu, C. Szymanski, J. McNeill, *Langmuir* **2006**, *22*, 2956.
- [46] E. J. Park, T. Erdem, V. Ibrahimova, S. Nizamoglu, H. V. Demir, D. Tuncel, *ACS Nano* **2011**, *5*, 2483.